# Two-color cesium magneto-optical trap with a ladder-type atomic system

**Baodong Yang (杨保东)[1,2,**], Jie Wang (王 杰)[1], and Junmin Wang (王军民)[1,*]**

[1]*State Key Laboratory of Quantum Optics and Quantum Optics Devices (Shanxi University), and Institute of Opto-Electronics, Shanxi University, Taiyuan 030006, China*

[2]*College of Physics and Electronic Engineering, Shanxi University, Taiyuan 030006, China*

**Corresponding author: wwjjmm@sxu.edu.cn; **Corresponding author: ybd@sxu.edu.cn*

Received October 23, 2015; accepted January 25, 2016; posted online March 1, 2016

We demonstrate a magneto-optical trap (MOT) with counter-propagating two-color cooling beams in a cesium $6S_{1/2} - 6P_{3/2} - 8S_{1/2}$ (852.3 + 794.6 nm) atomic system. Based on the conventional MOT due entirely to the 852.3 nm cooling laser's scattering forces, we replace one of the six 852.3 nm cooling beams with a 794.6 nm cooling beam. Our two-color MOT can efficiently cool and trap atoms from the red to blue detuning sides of two-photon resonance without pre-cooling. The technique is promising for the direct generation of correlated photon pairs in a two-color MOT based on diamond-configuration four-wave mixing.

*OCIS codes: 020.3320, 020.1670, 270.4180, 270.1670.*

*doi: 10.3788/COL201614.040201.*

Laser cooling and trapping of neutral atoms has played a fundamental role in a range of fields, from precision metrology and Bose–Einstein condensation to quantum information processing and so on. To date, most laser cooling techniques use the mechanical effect of the single-photon transition between a ground state and an excited state, such as the conventional magneto-optical trap (MOT)[1–3], polarization gradient cooling (PGC)[4], and velocity-selective coherent population trapping[5], but these methods seem more applicable to alkali-metal atoms. For the two-photon (or two-color) laser cooling in a ladder-type system comprising a ground state and two excited states, most theoretical and experimental studies are focused on the alkaline-earth-metal atoms with nondegenerate ground states and no hyperfine structure, and cooling with narrow $^1S_0 - {}^3P_1$ inter-combination transitions is often used as a second stage for a lower temperature after the initial pre-cooling milli-Kelvin temperatures by single-photon Doppler cooling with a strong $^1S_0 - {}^1P_1$ dipole transition. This is because the Doppler temperature limit is proportional to the linewidth of the transition[6–8]. Recently, a two-color MOT based on a cesium (Cs) $6S_{1/2} - 6P_{3/2} - 8S_{1/2}$ (852.3 + 794.6 nm) ladder-type system was experimentally demonstrated: a pair of 852.3 nm cooling beams along one of the axes in a conventional three-dimensional (3D) MOT was replaced with a pair of 794.6 nm cooling beams, which coupled the excited states $6P_{3/2} - 8S_{1/2}$ transition. It can efficiently cool and trap atoms on both the red and blue detuning sides of the two-photon resonance without pre-cooling[9,10]. One of the applications for this two-color MOT is the background-free fluorescence detection of trapped atoms[10]. More potential applications should be possible from the quantum coherence between the trapped atoms and cascaded two-color cooling lasers in this MOT[11–15].

In this Letter, we firstly demonstrate another two-color MOT configuration based on the Cs × $6S_{1/2} - 6P_{3/2} - 8S_{1/2}$ transitions, where the counter-propagating 852.3 and 794.6 nm cooling beams are along the axis of the anti-Helmholtz coil pair of the MOT, as shown in Fig. 1(a). Remarkably, our two-color MOT can cool and trap atoms ***from the negative to the positive detuning side*** of the two-photon resonance without pre-cooling in a vapor cell. One of the motivations for this work is to directly generate correlated photon pairs at 761.1 and 894.6 nm based on four-wave mixing (FWM) in a diamond-level atomic system, as shown in Fig. 1(b). The two-color cooling lasers simultaneously serve as the two pump beams in the FWM[16], and so this will greatly simplify the experimental setup. In aspect of the beam geometry for FWM, one of advantages of the two-color MOT configuration in this work is that the optical thickness of the trapped atoms is more fully utilized due to the nearly counter-propagating two-color cooling beams than the perpendicular cases in the previous two-color MOT

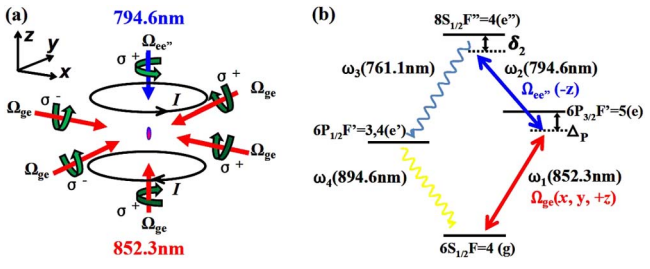


Fig. 1. (a) Schematic diagram of the laser beam arrangement for the two-color Cs MOT. The values of $\sigma^{\pm}$ are specified with respect to the positive $x$-, $y$-, and $z$-axes, and $I$ is the electric current of the anti-Helmholtz coils. (b) Simplified diagram of energy levels and related transitions.

 

configuration[9,10]. Furthermore, the counter-propagating geometry is often adopted to maximize the overlap region in the medium and Doppler selectivity in a diamond-configuration FWM experiment[16].

Our experimental setup has already been described in a previous work[10]. The frequency of an 852.3 nm cooling laser is locked to the $6S_{1/2}(F=4)-6P_{3/2}(F'=5)$ cycling transition with red detuning. The frequency of the 794.6 nm cooling laser can be offset locked by the off-resonant double-resonance optical-pumping spectrum ($\Delta_p+\Delta_c=0$, $\Delta_p$, and $\Delta_c$ are the detunings of the 852.3 and 794.6 nm lasers to the lower and upper transitions, respectively)[17,18], or by a two-color polarization spectrum[19,20]. The 852.3 nm repumping laser along the $\pm x$- and $\pm y$-axes is locked to the $6S_{1/2}(F=3)-6P_{3/2}(F'=4)$ transition, which keeps atoms in the $6S_{1/2}(F=4)$ ground state for continuously effective cooling. Figure 1(b) is the simplified level diagram and related transitions. $\Omega_{ge}$ and $\Omega_{ee''}$ are the Rabi frequencies of the 852.3 and 794.6 nm cooling lasers, $\Delta_p$ and $\delta_2$ are the single-photon and two-photon detunings for the $6S_{1/2}(F=4)-6P_{3/2}(F'=5)-8S_{1/2}(F''=4)$ cascaded transitions, and the linewidths for the $6P_{3/2}$ and $8S_{1/2}$ states are $\Gamma=5.2$ MHz and $\gamma=1.5$ MHz[9], respectively. The intensities of the 852.3 and 794.6 nm cooling beams are characterized by $S_{ge}=2\Omega_{ge}^2/\Gamma^2$ and $S_{ee''}=2\Omega_{ee''}^2/\gamma^2$. The helicity of the 794.6 nm cooling beam is set to be opposite to that of 852.3 nm cooling beam in a conventional 3D MOT, as indicated in Fig. 1(a).

Figure 2 shows typical experimental results for our two-color MOT. When the single-photon detuning of a 852.3 nm cooling laser $\Delta_P=-10$ MHz $\sim 2\Gamma$, we find that this two-color MOT can efficiently cool and trap atoms from the negative to positive two-photon detuning. With the negative two-photon detuning, the cooling mechanism can be understood by using a two-photon Doppler cooling picture, which is similar to that of a conventional 3D MOT. With positive two-photon detuning, the cooling mechanism may be explained using a two-color PGC picture or coherent cooling[9,12–14]. It is worth mentioning again that our two-color MOT also can trap atoms at the two-photon resonant point $\delta_2=0$, as shown in Fig. 2(a). However, this characteristic phenomenon has not easily been observed in previous two-color MOTs[9,10]. This counterintuitive experimental result has been proven to be objective by repeating the measurements twice under the same experimental parameters (each data point in Fig. 2 is averaged data from three measurements). This interesting phenomenon may be explained by the fact that the cold atoms (their velocity components along the $x$- and $y$-axes are fully decreased by 852.3 nm cooling beams, and some near-zero velocity component of these atoms in a dimensional Maxwell–Boltzmann velocity distribution along the $z$-axis is selected and shelved in a dark state) are gathered in a superposition dark state induced by the ladder-type electromagnetically induced transparency when $\delta_2=0$ for the counter-propagating 852.3 and 794.6 nm cooling beams[12–14,21,22]. Typical experimental parameters

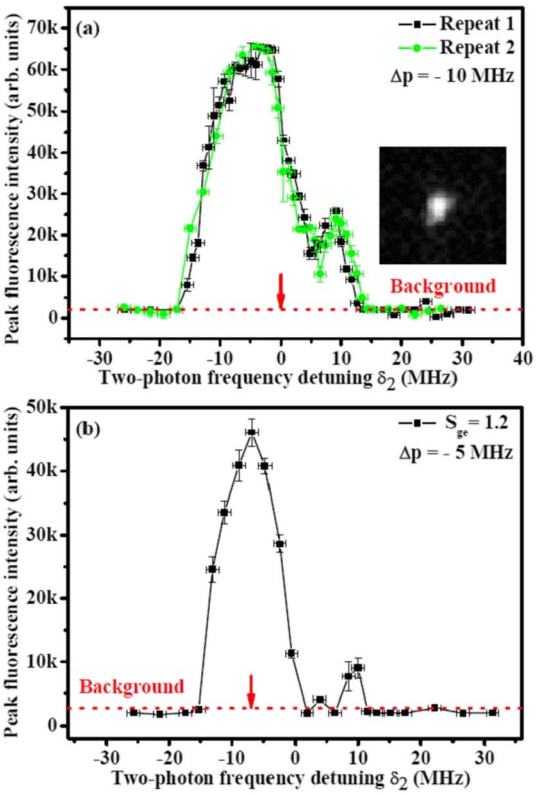


Fig. 2. Peak fluorescence intensity of the trapped atoms versus two-photon frequency detuning $\delta_2$ under the condition of (a) $\Delta_P=-10$ and (b) $-5$ MHz. The vertical error bars signify the standard deviation of several measurements, and the horizontal error bars denote the uncertainty of the frequency fluctuation with $\sim\pm 1$ MHz after laser locking. The inset in (a) gives a typical fluorescence picture of a cold atoms cloud at $\delta_2=-9$ MHz by a charge-coupled device camera.

are as follows: the intensity of cooling beams along the $\pm x$ directions: $\sim 2\times 14\,\mathrm{mW/cm^2}$@852.3 nm($S_{ge}\sim 2\times 13$), along the $\pm y$ directions: $\sim 2\times 14\,\mathrm{mW/cm^2}$@852.3 nm($S_{ge}\sim 2\times 13$), along the $\pm z$ directions: $\sim 2.2\,\mathrm{mW/cm^2}$@852.3 nm+$\sim 58.7\,\mathrm{mW/cm^2}$@794.6 nm ($S_{ge}\sim 2+S_{ee''}\sim 44$); the intensity of repumping beams along the $\pm x$ and $\pm y$ directions: $\sim 4\times 3.9$ mW/cm$^2$@852.3 nm; the $1/e^2$ diameters of cooling and repumping beams are $\sim 6$ mm; the typical gradient of the quadruple magnetic field is $\sim 10$ Gauss/cm, and the typical pressure in a vacuum chamber with released Cs atoms is $\sim 6.6\times 10^{-6}$ Pa. When $\Delta_P=-5$ MHz $\sim\Gamma$, which is closer then the $6S_{1/2}(F=4)-6P_{3/2}(F'=5)$ transition, the collisional heating induced by the single-photon and cascaded two-photon transitions will become serious, and simultaneously leads to the decay of dark state, so it will become difficult to efficiently trap atoms at $\delta_2=0$, as shown in Fig. 2(b). Figure 2(b) was measured at the optimized intensity 1.3 mW/cm$^2$ ($S_{ge}\sim 1.2$) of 852.3 nm cooling beam along the $+z$-axis for more trapped atoms, and the other parameters are the same as in Fig. 2(a).

For many applications, samples of cold and dense atoms are often desired. Unfortunately, the number of trapped

atoms in the two-color MOT is an order of magnitude smaller than that of a conventional 3D MOT. One of main reasons is that the capture velocity $v_c$ along the $z$-axis is obviously reduced because $v_c \propto \gamma^3$[23], where the atoms populated in the intermediate state $6P_{3/2}$ with linewidth $\Gamma = 5.2$ MHz are further coupled to another higher excited state $8S_{1/2}$ with a narrower linewidth $\gamma = 1.5$ MHz via the 794.6 nm cooling laser. For the purpose of trapping more atoms in a conventional 3D MOT, a popular method is to strengthen the intensity of the cooling laser. However, we found that the peak fluorescence of the trapped atoms (approximately proportional to the number of trapped atoms) in our two-color MOT increases at first and then descends with the increasing 852.3 nm cooling laser intensity along the $z$-axis whenever $\delta_2 = -6.5$ or $+8.8$ MHz, as shown in Fig. 3(a). There are several reasons for these changing trends: (1) one obvious reason is the unbalance of radiation pressure from the counter-propagating 852.3 nm cooling beam with the changed intensity and the 794.6 nm cooling beam with a fixed intensity $S_{ee''} \sim 44$ along the $z$ direction, which will be further indicated in Fig. 4; (2) another latent and very important reason is cold collisions[23–25], because we have observed the same changing trends in previous two-color MOTs with a pair of counter-propagating 794.6 nm cooling beams, although their radiation pressure from the $\pm z$ directions is balanced. According to the changes of the internal states of the colliding atoms, the collisions are classified into a hyperfine-structure-changing collision between two ground state atoms, and a fine-structure change and radiative escape between a ground state atom and an excited atom. These collision processes lead to the same changing trends in a conventional 3D MOT[23–25] as that in the Fig. 3(a). For the two-color MOT, it is necessary to further take account of the atom collisions between the excited states $6P_{3/2}$ and $8S_{1/2}$ with the assistance of the 794.6 nm cooling beams. Unfortunately, the study of the collisions involving two excited atoms has been given little attention, and this may increase the collisional loss for their higher energy. Thus, when the detuning of the 852.3 nm cooling laser $\Delta_P = -5$ MHz is closer to the $6S_{1/2}(F = 4) - 6P_{3/2}(F' = 5)$ cooling transition, more atoms will be populated on the excited state $6P_{3/2}(F' = 5)$, and a more intensive collisional loss makes it more difficult for a two-color MOT to trap atoms around $\delta_2 = 0$, as shown in Fig. 2(b). (3) Another reason is the coherent cooling between the two-color cooling lasers and atoms in this ladder-type MOT, which is mainly responsible for the cooling at the $\delta_2 > 0$. With the increase of the 852.3 nm cooling laser intensity, the coherence of the atomic system must be gradually destroyed by the

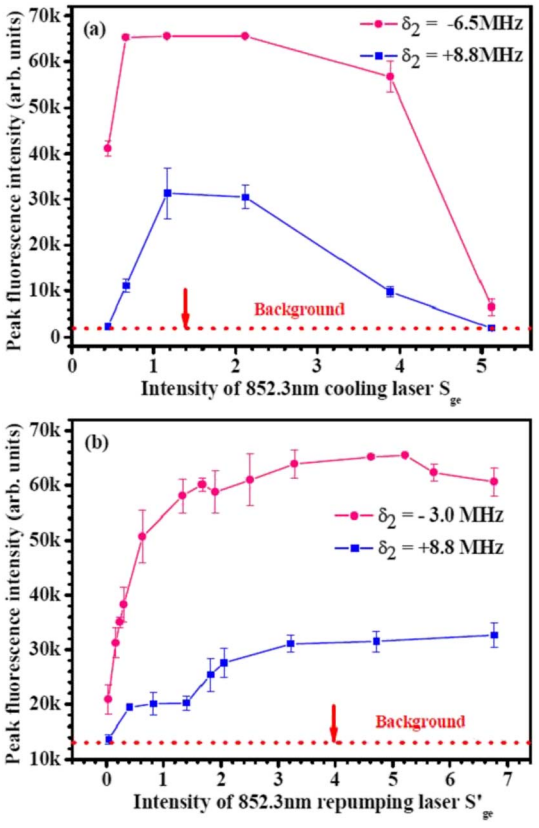


Fig. 3. Peak fluorescence intensity of trapped atoms versus intensity of (a) 852.3 nm cooling laser and (b) repumping laser. The error bars signify the standard deviation of several measurements.

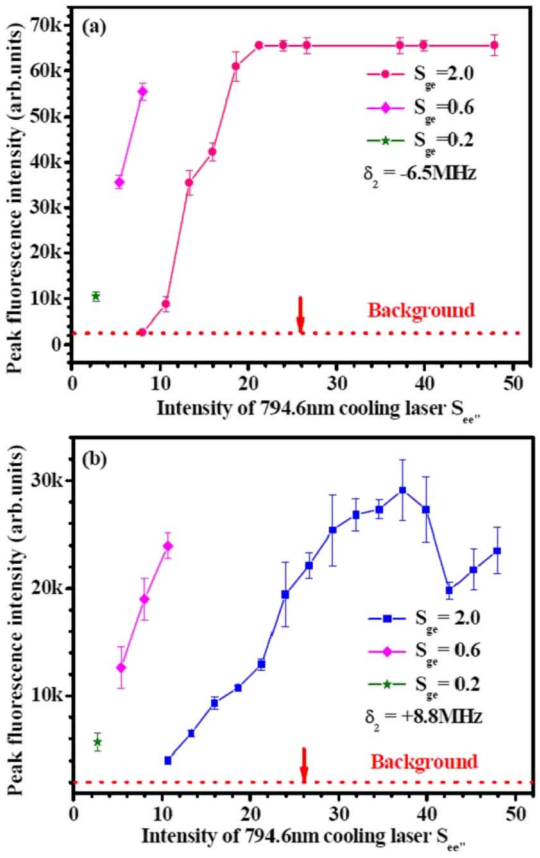


Fig. 4. Peak fluorescence intensity of trapped atoms versus intensity of 794.6 nm cooling laser for the two-photon detuning (a) $\delta_2 = -6.5$ and (b) $+8.8$ MHz. The error bars signify the standard deviation of several measurements.

spontaneous decay, so that the effect of coherent cooling is suppressed at a certain degree. This is the reason that the number of trapped atoms more rapidly declines at $\delta_2 = +8.8$ MHz than at $\delta_2 = -6.5$ MHz, where there exists two-photon Doppler cooling and coherent cooling mechanisms, as shown in Fig. 3(a)[12–14,21,22]. Another piece of experimental proof for the coherence effect is that the range of the 852.3 nm cooling laser intensity for trapping atoms is enlarged when increasing the 794.6 nm cooling laser intensity at $\delta_2 = -3.0$ MHz, because the intensive 794.6 nm cooling laser makes the 852.3 nm cooling laser transparent due to quantum coherence[21,22], and suppresses collisional loss involving excited states to some extent. Among the above three reasons, the cold collisional loss governs the whole tendency in Fig. 3(a), which is also suitable to the previous two-color MOT[9,10]; quantum coherence will influence the tendency to a certain degree based on the suppression of collisional loss. There exists the unbalance of radiation pressure, which is fully demonstrated in Fig. 4. But the unbalance can be compensated by the quadruple magnetic field, because the atoms always look for a new, balanced position near the center of the gradient of the quadruple magnetic field when changing the intensity of the cooling lasers.

During the cooling process of a two-color MOT with the unclosed $6S_{1/2}(F=4) - 6P_{3/2}(F'=5) - 8S_{1/2}(F''=4)$ cooling transitions, the atoms will be pumped into the $6S_{1/2}(F=3)$ ground state via the other intermediate states, such as $6P_{3/2}(F'=4,3)$ by single- and double-resonance optical pumping[21]. Thus, for the continuous and efficient cooling of a two-color MOT, the repumping laser will be important to pump atoms back to the $6S_{1/2}(F=4)$ ground state from the $6S_{1/2}(F=3)$ state. Figure 3(b) presents the changes of peak fluorescence of the trapped atoms versus the intensity of the 852.3 nm repumping laser; the peak fluorescence intensity reaches saturation levels at the repumping laser intensity $S'_{ge} = \sim 2.0$ for $\delta_2 = -3.0$ and $+8.8$ MHz.

Different from the influence of the 852.3 nm cooling laser intensity, the number of trapped atoms generally increases with the increase of the 794.6 nm cooling laser intensity, as shown in Fig. 4. This is because a collisional loss involving excited states is limited by the exciting probability of the ground state $6S_{1/2}$ to intermediate state $6P_{3/2}$ for a fixed 852.3 nm cooling laser intensity even if the 794.6 nm cooling laser intensity increases. Furthermore, the intensive 794.6 nm cooling laser will suppress this collisional loss due to the coherence effect as shown in Fig. 3(a). In addition, we found that the 794.6 nm cooling laser intensity is in the range of $S_{ee''} = \sim 2.6$–$50.6$; this MOT all can trap atoms at $\delta_2 = -6.5$ and $+8.8$ MHz. For the sake of the balance of the radiation pressure between the 852.3 and 794.6 nm cooling beams along the $z$-axis, when the intensity of the 794.6 nm cooling laser becomes small, the intensity of 852.3 nm cooling laser also is correspondingly reduced, as when, for example, $S_{ge} = \sim 0.2 (\sim 0.23\ \mathrm{mW/cm^2})$, as indicated in Fig. 4. These changes are very different from the previous two-color MOT with a pair of counter-propagating 794.6 nm cooling beams[9,10], which can trap atoms at the $\delta_2 > 0$ only when the 794.6 nm cooling laser intensity is larger than a threshold value $S_{ee''} > \sim 34$ in our experiment. Compared with the previous two-color MOT, the two-color MOT in this work can trap atoms over a wide range of the 794.6 nm cooling laser's intensity.

In conclusion, we demonstrate an MOT with counter-propagating two-color cooling laser beams in an experiment, and also measure and analyze the influence of the cooling laser intensity, the repumping laser intensity, and the frequency detuning of this two-color MOT. The experimental results show that this two-color MOT can be more easily realized compared with the previous two-color MOT configuration, because the MOT in this work can trap atoms from the negative to positive two-photon detuning (including $\delta_2 = 0$), and also there seems not to be a threshold value of the 794.6 nm cooling laser intensity for trapping atoms at the positive two-photon detuning. In addition, our scheme provides a very flexible experimental configuration for the two-color MOT. Any one of the 852.3 nm cooling beams in a conventional 3D MOT can be replaced with a 794.6 nm cooling beam, in principle. It is convenient for the integration of the preparation of cold atoms and the generation of correlated photon pairs, even correlated beams, based on the FWM process. The technique also may be extended to the laser cooling of Rydberg atoms in a cascaded atomic configuration, although it has a long lifetime[26,27]. We believe these investigations and techniques are helpful for a deeper understanding of the two-color MOT and its many applications.

This work was financially supported by the National Major Scientific Research Program of China (No. 2012CB921601), the National Natural Science Foundation of China (Nos. 11104172, 11274213, and 61475091), and the Research Program for Sci and Tech Star of Tai Yuan, Shanxi Province, China (No. 12024707).

## References

1. W. D. Phillips, Rev. Mod. Phys. **70**, 721 (1998).
2. Q. Qu, B. Wang, D. Lü, J. Zhao, M. Ye, W. Ren, J. Xiang, and L. Liu, Chin. Opt. Lett. **13**, 061405 (2015).
3. X. Wang, H. Cheng, L. Xiao, B. Zheng, Y. Meng, L. Liu, and Y. Wang, Chin. Opt. Lett. **10**, 080201 (2012).
4. J. Dalibard and C. Cohen-Tannoudji, J. Opt. Soc. Am. B **6**, 2023 (1989).
5. J. Hack, L. Liu, M. Olshanii, and H. Metcalf, Phys. Rev. A **62**, 013405 (2000).
6. E. A. Curtis, C. W. Oates, and L. Hollberg, Phys. Rev. A **64**, 031403 (R) (2001).
7. W. C. Magno, R. L. Cavasso Filho, and F. C. Cruz, Phys. Rev. A **67**, 043407 (2003).
8. N. Malossi, S. Damkjær, P. L. Hansen, L. B. Jacobsen, L. Kindt, S. Sauge, and J. W. Thomsen, Phys. Rev. A **72**, 051403(R) (2005).
9. S. J. Wu, T. Plisson, R. C. Brown, W. D. Phillips, and J. V. Porto, Phys. Rev. Lett. **103**, 173003 (2009).

10. B. D. Yang, Q. B. Liang, J. He, and J. M. Wang, Opt. Express **20**, 11944 (2012).
11. R. Y. Chang, W. C. Fang, B. C. Ke, Z. S. He, M. D. Tsai, Y. C. Lee, and C. C. Tsai, Phys. Rev. A **76**, 055404 (2007).
12. G. Morigi and E. Arimondo, Phys. Rev. A **75**, 051404(R) (2007).
13. F. Schmidt-Kaler, J. Eschner, G. Morigi, C. F. Roos, D. Leibfried, A. Mundt, and R. Blatt, Appl. Phys. B **73**, 807 (2001).
14. C. Fort, F. S. Cataliotti, M. Prevedelli, and M. Inguscio, Opt. Lett. **22**, 1107 (1997).
15. R. Cao, B. Gai, J. Yang, T. Liu, J. Liu, S. Hu, J. Guo, Y. Tan, S. He, W. Liu, H. Cai, and X. Zhang, Chin. Opt. Lett. **13**, 121903 (2015).
16. D. A. Braje, V. Balic, S. Goda, G. Y. Yin, and S. E. Harris, Phys. Rev. Lett. **93**, 183601 (2004).
17. H. S. Moon, W. K. Lee, L. Lee, and J. B. Kim, Appl. Phys. Lett. **85**, 3965 (2004).
18. B. D. Yang, J. Y. Zhao, T. C. Zhang, and J. M. Wang, J. Phys. D: Appl. Phys. **42**, 085111 (2009).
19. C. Carr, C. S. Adams, and K. J. Weatherill, Opt. Lett. **37**, 118 (2012).
20. B. D. Yang, J. Wang, H. F. Liu, J. He, and J. M. Wang, Opt. Commun. **319**, 174 (2014).
21. B. D. Yang, Q. B. Liang, J. He, T. C. Zhang, and J. M. Wang, Phys. Rev. A **81**, 043803 (2010).
22. B. D. Yang, J. Gao, T. C. Zhang, and J. M. Wang, Phys. Rev. A **83**, 013818 (2011).
23. M. S. Santos, P. Nussenzveig, A. Antunes, P. S. P. Cardona, and V. S. Bagnato, Phys. Rev. A **60**, 3892 (1999).
24. C. D. Wallace, T. P. Dinneen, K. N. Tan, T. T. Grove, and P. L. Gould, Phys. Rev. Lett. **69**, 897 (1992).
25. S. R. Muniz, K. M. F. Magalhães, Ph. W. Courteille, M. A. Perez, L. G. Marcassa, and V. S. Bagnato, Phys. Rev. A **65**, 015402 (2001).
26. J. Guo, E. Korsunsky, and E. Arimondo, Quant. Semiclass. Opt. **8**, 557 (1996).
27. A. K. Mohapatra, T. R. Jackson, and C. S. Adams, Phys. Rev. Lett. **98**, 113003 (2007).